 CMC, vol.52, no.2, pp.105-121, 2016

Effects of Stacking Sequence and Impactor Diameter on Impact Damage of Glass Fiber Reinforced Aluminum Alloy Laminate

Zhengong Zhou[1], **Shuang Tian**[1,2] **and Jiawei Zhang**[3]

Abstract: The methods of numerical simulation and test are combined to analyze the impact behavior of glass fiber reinforced aluminum alloy laminate (GLARE). A new failure criteria is proposed to obtain the impact failure of GLARE, and combined with material progressive damage method by writing code of LS-DYNA. Low velocity impact test of GLARE is employed to validate the feasibility of the finite element model established. The simulation results have been shown that progressive damage finite element model established is reliable. Through the application of the finite element model established, the delamination of GLARE evolution progress is simulated, various failure modes of GLARE during impact are obtained, and the effects of stacking sequence and impactor diameter on the impact damage of GLARE are obtained.

Keywords: GLARE, Impact behavior, Progressive damage, Finite element method, Impact test.

1 Introduction

Glass fiber reinforced aluminum alloy laminate (GLARE) as a kind of fiber metal laminate (FML) is made of aluminium alloy sheet and alterable stacking sequence of glass fiber reinforced composites, which was first applied to cabin in 1987, and then widely adopted in practical engineering seen Volt (1996, 1999, 2011) and Straznicky (2000). GLARE combine the advantages of aluminum alloy with glass fiber reinforced composites, becomes a structural material with low density, good corrosion resistance and impact resistance seen Sinmazçelik (2011) and Wu and Yang (2005). Damage and failure of aircraft structures caused by impact has been investigated over the years. Studies show that aviation structural failure problems

[1] Center for Composite Materials, Harbin Institute of Technology, Harbin, China
[2] Corresponding author E-mail: hit_ts@163.com
[3] Beijing Institute of Mechanical Equipment, Beijing, P. R. China

always caused by impacting seen Vogelesang (2000). Therefore, it is necessary to acquire knowledge concerning impact damage tolerance of structural materials. By means of test and numerical simulation, researchers have attained a number of achievements currently. In respect of test, impact tests usually conducted after laminates are clamped or simply supported seen Pang (1991), Pierson (1996) and Lee (1997). Because the plastic deformation of the aluminum alloy after impact, the damage inspection of fiber reinforced aluminum alloy laminate (FML) test focuses on the superficial phenomena observation. These studies include the analysis of the influence of impactor size, specimen geometry shape and composite stacking sequence on impact damage of FML seen Liu (2010) and Abdullah (2006). In the respect of simulation, researchers have been working for establishing an appropriate analytical model to simulate the composite laminate, such as a simple locking-alleviated 3D 8-node mixed-collocation C-0 finite element and a simple locking-alleviated 4-node mixed-collocation C-0 finite element are developed in Dong's study (2014). A majority of researchers employed commercial analytical software such as ABAQUS and LS-DYNA, however, the judgment for composite failure mode in the software cannot describe the complicated three-dimensional impact problem accurately. In order to overcome this disadvantage, the user subroutine was developed. Tita (2008) developed a Vectorized User Material Subroutine (VUMAT) to simulate the impact damage of CFRP laminates. In his simulation the different failure criterias seen Yamada (1978) and Hashin (1979) are employed in ABAQUS software by VUMAT. In modeling, considering interface delamination is an important failure mode in impact, the cohesive element as a special kind of finite elements used to model the interfacial layers in laminates. The mechanical behavior of these elements depend on the kind of constitutive relations implemented while analysis seen Sosa (2012).

So far, Many researchers have attempted to model the low-velocity impact response and capture the various failure modes seen Faggiani (2010), Zhou (2012), Zhou (2006), and Foo (2011). The overall findings was reviewed in Chai's (2011). But the failure mode of delamination established before ignore the shear stress influence of neighboring layers on interface layer, and the material performance is progressive degradation during impact, but always regard as damage when failure initial. For these reasons, a new failure criterion of composites by modifying Hou's is proposed in this paper. The new failure criterion include five failure modes of composites, consider the shear stress effect of neighboring layers on interface layer, and distinct different failure modes of fiber. By subroutine code combine the new failure criterion with the material performance progressive degradation method, which is employed to analyze the impact behavior of GLARE. Through the simulation, the internal damage evolution process of GLARE during the impact is obtained, and

the effects of stacking sequence and impactor diameter on the impact resistance of GLARE are also obtained.

2 Impact tests and finite element model

In order to analyze the phenomena of GLARE during impact test, nonlinear finite element analysis software LS-DYNA is employed. The general steps involved to model the complex phenomenon are explained via a flowchart shown in **Figure 1**. The development module in **Figure 1** is achieved by writing subroutine code into computational process. The original module is existing module of software, which can be employed directly.

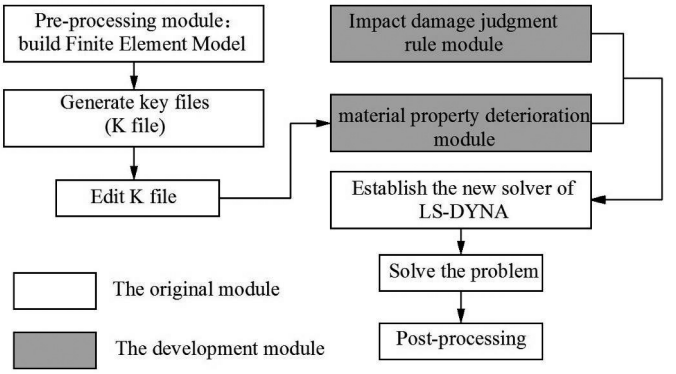

Figure 1: Finite element simulation process

2.1 Material model to analyze the impact failure of GLARE

In order to obtain dynamic behavior of GLARE during impact, choosing suitable failure modes to acquire all possible failure of composite layer and plasticity effect of aluminum alloy layer is necessary. GLARE is covered with aluminum alloy layer, its stress and strain relationship during impact can be analyzed with Johnson Cook Plasticity Model (J-C) seen Kashani (2015) as follows:

$$\sigma_y = (A + B\bar{\varepsilon}^{pn})(1 + c\ln\dot{\varepsilon}^*)(1 - T^{*m}) \tag{1}$$

In the formula, A is the yield stress, B and n represent effects of strain hardening; $\bar{\varepsilon}^p$ is equivalent plastic strain; c is strain rate constant; $\dot{\varepsilon}^* = \dot{\varepsilon}/\dot{\varepsilon}_0$ is dimensionless plastic strain rate for $\dot{\varepsilon}_0 = 1\text{s}^{-1}$; $T^* = (T - T_{room})/(T_{melt} - T_{room})$ is homologous temperature, in which, T_{melt} is melt temperature and T_{room} is room temperature; m is melt temperature index. As presented in formula (1), by means of multiplying,

the strain hardening, strain rate and temperature are taken into consideration in the model. Besides, the three considered are mutually independent. So this model is applicable to metal material analysis in impact. In a J-C model, metal damage failure criterion is expressed as follows:

$$\varepsilon^f = [d_1 + d_2 \exp \mathrm{d}_3 \sigma^*][1 + d_4 \ln \varepsilon^*][1 + d_5 T^*] \tag{2}$$

In formula (2), $\sigma^* = p/\sigma^y$, p is the material pressure; The value of $d_i (i = 1, \ldots, 5)$ are constant, can be obtained by testing. Because 2024-T3 aluminum alloy is adopted in this paper, the performance parameters adopt the test results of Kay (2002) as shown in **Table 1**. During calculating, the value of $\Delta\bar{\varepsilon}^p/\bar{\varepsilon}^p$ is obtained, the failure induced when the value increase to 1, or else the material is considered to be intact, circular calculation is conducted.

Table 1: 2024-T3 aluminum alloy sheet performance parameter seen Kay (2002)

Elastic parameters	$E = 724GPa$, $\nu = 0.33$, $\rho = 2770kg/m^3$
The yield parameters	$A = 265MPa$, $B = 426MPa$, $c = 0.015$, $m = 1$, $n = 0.34$
Failure parameters	$d_1 = 0.13, d_2 = 0.13, d_3 = -1.5, d_4 = 0.011$

During impact, various failure modes of glass fiber reinforced composite inside GLARE will be induced, and the failure mode and evolution process are complex. In this paper five kinds of composite failure modes are taken into consideration, such as matrix cracking, matrix crushing, fiber tensile breakage, fiber compression breakage and interface delamination. The strength failure criterion proposed by Hou (2000) is considered to analyze the generation of failure. The failure criterions concerning the matrix are presented as follows:

Matrix cracking:

$$e_m^2 = \left(\frac{\sigma_{22}}{Y_T}\right)^2 + \left(\frac{\sigma_{12}}{S_{12}}\right)^2 + \left(\frac{\sigma_{23}}{S_{23}}\right)^2 \geq 1, (\sigma_{22} \geq 0) \tag{3}$$

Matrix crushing:

$$e_d^2 = \frac{1}{4}\left(\frac{-\sigma_{22}}{S_{12}}\right)^2 + \frac{Y_C^2 \sigma_{22}}{4S_{12}^2 Y_C} - \frac{\sigma_{22}}{Y_C} + \left(\frac{\sigma_{12}}{S_{12}}\right)^2 \geq 1, (\sigma_{22} < 0) \tag{4}$$

When analyzing fiber failure, Hou ignored different failure modes of impact surface and back. Therefore, two different failure modes of fiber tensile and fiber compression are taken into consideration in this paper, and the expressions below are adopted to analyze fiber failure:

Fiber compression failure:

$$f_c^2 = \left(\frac{\sigma_{11}}{X_C}\right)^2 + \left(\frac{\sigma_{12}}{S_f}\right)^2 + \left(\frac{\sigma_{13}}{S_f}\right)^2 \geq 1, (\sigma_{11} < 0) \tag{5}$$

Fiber tensile failure:

$$f_t^2 = \left(\frac{\sigma_{11}}{X_T}\right)^2 + \left(\frac{\sigma_{12}}{S_f}\right)^2 + \left(\frac{\sigma_{13}}{S_f}\right)^2 \geq 1, (\sigma_{11} \geq 0) \tag{6}$$

During the impact, delamination is one of the main failure mode seen Chai (2014). During modeling, between the prepreg layers is introduced the interface element to simulate the delamination. Because of the delamination criterion which Hou proposed ignored the effect of neighbor layers shear on interface. Therefore, a new delamination failure criterion is proposed as follows:

Interface delamination:

$$e_l^2 = \left(\frac{{}^{n}\sigma_{23}}{S_{l23}}\right)^2 + \left(\frac{{}^{n+1}\sigma_{23}}{S_{l23}}\right)^2 + \left(\frac{\sigma_{33}}{Z_T}\right)^2 + \left(\frac{\sigma_{22}}{Y_T}\right)^2 \geq 1, (\sigma_{33} \geq 0) \tag{7}$$

Where σ_{11} is stress in the fiber direction; σ_{22} is stress in the transverse direction; σ_{33} is stress in the thickness direction; σ_{12} is shear stress in fiber and transverse directions; σ_{23} is shear stress in transverse and thickness directions; σ_{13} is shear stress in fiber and thickness directions; X_T is tensile strength in fiber direction; X_C is compressive strength in fiber direction; Y_T is tensile strength in transverse direction; Y_C is compressive strength in transverse direction; Z_T is tensile strength in thickness direction; S_{12} is shear strength in fiber and transverse directions; S_{23} is shear strength in transverse and thickness directions; S_f is shear strength of fiber failure; S_{l23} is shear strength for delamination in transverse and thickness directions; n is the number of layers of the laminates.

During numerical simulation, when any stress calculation result of element satisfied the criterions (3)–(7), the element is considered occur the failure mode accordingly, then the failure element performance degradation will happen.

2.2 Obtain the material degradation parameter

In order to obtain accurate simulation results, it is important to select suitable degradation model of composite. In this section, the degradation model of composite proposed by Kermanidis (2000) is employed. Through a lot of contrast analysis between simulation results and test results, the material property degradation values of glass fiber reinforced composite inside the GLARE are obtained.

2.2.1 Low velocity impact test

Low velocity impact test is conducted with drop hammer impact test machine in this paper. The impactor head is a hemisphere with 8mm diameter, and impactor mass is 11kg. The tests are conducted for two kinds of GLARE with the initial impact energy of 25J. The stacking sequence of produced GLARE specimens are unidirectional (Al/0/0/0/0/Al) and symmetric orthotropic laminates (Al/0/90/90/0/Al). Performance parameters of aluminum alloy sheet and glass fiber reinforced composite single-layer laminate are shown **Table 1** and **Table 2**. In the process of specimen production, firstly decontaminate the aluminum alloy sheet in acetone solution, then degrease in alkali solution, then deoxidize in nitric acid solution, then anodize in phosphoric acid solution, then clean and dry. Secondly lay the glass fiber reinforced prepreg according to **Table 3**, then put into a vacuum tank for heating and curing. Finally take it out until cool to ambient temperature, and cut it into specimens size with water jet cutting machine. The dimensions of specimen are shown in **Table 3**.

Table 2: Glass fiber reinforced composite laminate performance parameters

Elastic parameters						Strength parameters			
$E_{11}(GPa)$	49.7	$G_{12}(GPa)$	5.3	ν_{12}	0.29	$S_T(MPa)$	65.5	$X_C(GPa)$	0.643
$E_{22}(GPa)$	12.9	$G_{13}(GPa)$	5.3	ν_{13}	0.29	$S(MPa)$	53	$Y_T(MPa)$	45.5
$E_{33}(GPa)$	12.9	$G_{23}(GPa)$	4.8	ν_{23}	0.29	$X_T(GPa)$	1.721	$X_C(MPa)$	131.1

Table 3: The dimensions size of GLARE test specimen

	t_{Al} (mm)	t_{GFP} (mm)	L (mm)	w (mm)
Al/0/90/90/0/Al	1	0.15	100	100

(Symbols in the table means: t = thickness, L = length, w = width)

2.2.2 Material property degradation method

In order to obtain composite degradation parameter, the finite element simulation results are compared with the tests, and three-dimensional finite element analysis model is established as shown in **Figure 2**. In the analytical model, impactor is made of rigid materials, and its elastic modulus is 210Gpa; Poisson's ratio is 0.3; density is 7800kg/m^3. Surface-to-surface contact condition is set between layers, as well as the impactor and every layer of laminate. The interpenetration between grids is not allowed. To guarantee that the impactor is perpendicular to laminate

surface during the impact, all freedom degrees of the impactor were limited, except the perpendicular direction. Besides, clamping around GLARE was defined as a fixed constraint. As GLARE is subject to short-term local stress impact, the grids of the impact region was refined. Failure criterions in section 2.1 are adopted in modeling to determine composite failure mode. Through comparative analysis, following composite degradation parameters of materials are employed:

Matrix cracking failure: E_{22}, G_{12}, G_{23} degrade to 0.4 of its original value;

Matrix crushing failure: E_{22}, G_{12}, G_{23} degrade to 0.5 of its original value;

Fiber compression failure: E_{11}, E_{22}, G_{12}, G_{23}, G_{13}, ν_{12}, ν_{23}, ν_{13} degrade to 0.18 of its original value;

Fiber tensile failure: E_{11}, E_{22}, G_{12}, G_{23}, G_{13}, ν_{12}, ν_{23}, ν_{13} degrade to 0.1 of its original value;

Interface delamination failure: E_{33}, G_{13}, E_{23}, ν_{13}, ν_{23} degrade to 0.

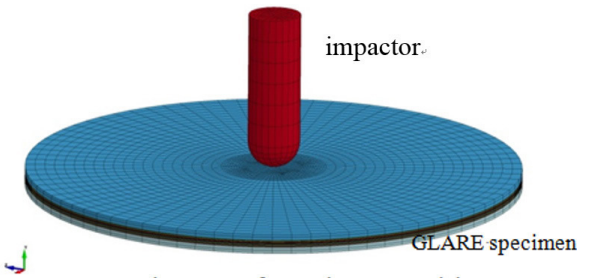

Figure 2: The finite element model of low velocity impact

2.3 Contrastive analysis of finite element simulation and test results

In order to validate the finite element model established is reliable, simulation is conducted with impact test conditions. During the simulation, stress analytical results of all elements are extracted for judging failure mode. The failure elements of aluminum alloy sheet can be determined with the formula (2). When the value of formula (2) reaches 1, aluminum alloy is considered to be failure, and failure elements should be removed. Otherwise, increase computational time steps, conduct stress analysis and failure judge again until the stress does not increase, then calculation is terminated. The failure element of glass fiber reinforced composites can be determined with the formula (3) to formula (7). When any of the formulas value reaches 1, materials property degradation is carried out in corresponding failure element as section 2.2.2. Otherwise, increase computational time steps, determine element stress and material degradation again until the stress does not increase. By

simulation, the typical load-displacement curves are obtained as shown in **Figure 3**.

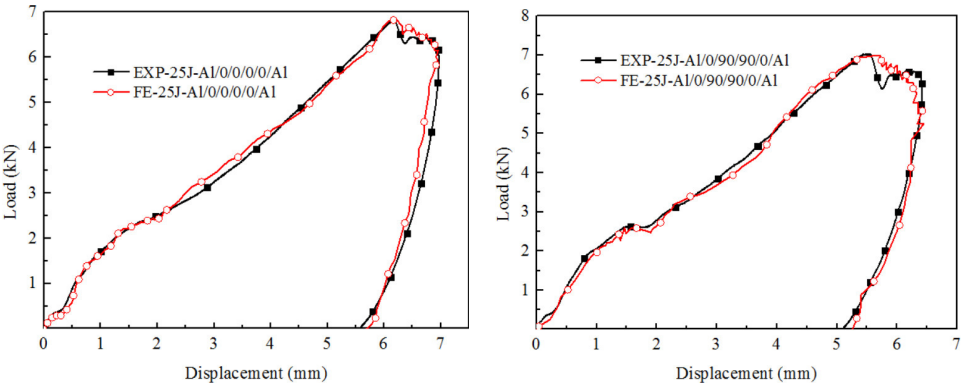

Figure 3: Load vs displacement curve of specimens under 25J impact. a) Al/0/0/0/0/Al GLARE, b) Al/0/90/90/0/Al GLARE.

It can be seen that results of simulation are in good agreement with that of experiment. Each load and displacement curve is divided into two stages of load and unload in the impacting. In Figure 3(a) and (b), it can be seen that the curve during unload stage is not smooth, which are caused by material failure. In addition, it can be seen that numerical simulation results are higher than test results, which is caused by simplifying assumptions during simulation analysis, such as fiber and resin are well bonded, as well as layers, but relative error is less than 10%, so results are reliable.

In order to obtain various failure modes of GLARE during impact accurately. The simulation results of GLARE after impact are compared with tests as shown in **Figure 4**. Through the comparison between **Figure 4**(a1) and (a2), **Figure 4**(b1) and (b2), results show that the finite element model adopted are suitable. The impact back of undirectional laminate as shown in **Figure 4** (a1) and (a2) has a 13mm line-shaped crack, which is consistent with the laying direction of prepreg. The impact back of symmetric orthotropic laminate as shown in **Figure 4**(b1) and (b2) has two mutual perpendicular cracks, of which, the longer crack is consistent with the impact back laying direction of prepreg with a length of 10mm, and the shorter crack that is perpendicular to the longer one is 5mm. Different cracks of the two specimens are caused by different stacking sequences of glass fiber reinforced composites inside GLARE.

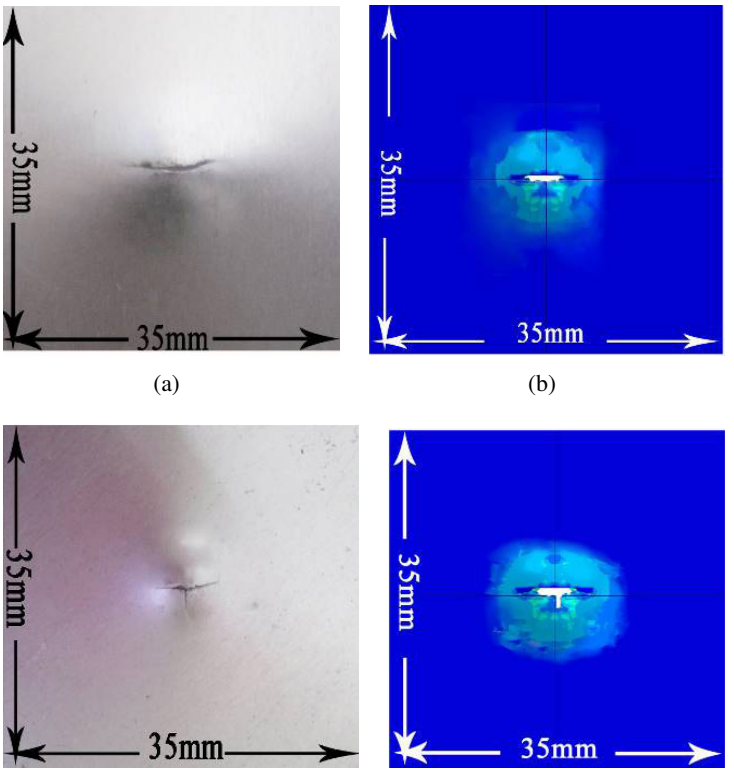

(a) (b)

(c) (d)

Figure 4: Failure modes of GLARE backs under 25J impact. The fiber direction of impact back is 0°, a) Al/0/0/0/0/Al back failure mode of specimen, b) Al/0/0/0/0/Al back failure mode of simulation, c) Al/0/90/90/0/Al back failure mode of specimen, b) Al/0/90/90/0/Al back failure mode of simulation

To analyze the damage of glass fiber reinforced composites inside GLARE during impact, aluminum alloy of GLARE after impact are removed in concentrated alkaline solution. The photos are shown in **Figure 5**(a) and **Figure 5**(c). The same impact simulation results are shown in **Figure 5**(b) and **Figure 5**(d). By comparing the simulation results and test results of two specimens, the results show that the failure criterion established in this paper are reliability. The result show that the internal damage shape of Al/0/0/0/0/AL is an oval, which major axis is in the fiber direction, and its main damage mode is matrix cracking. The internal damage shape of Al/0/90/90/0/AL is a cross, and its main damage mode is interfacial delamination. These phenomenon above are induced by different stacking sequences, and shear stress of neighbor layers influence interface delamination. Therefore, the

delamination criterion proposed in this paper is suitable. Through the comparison between simulation and test results, demonstrate that the finite element model established is reliable and effective.

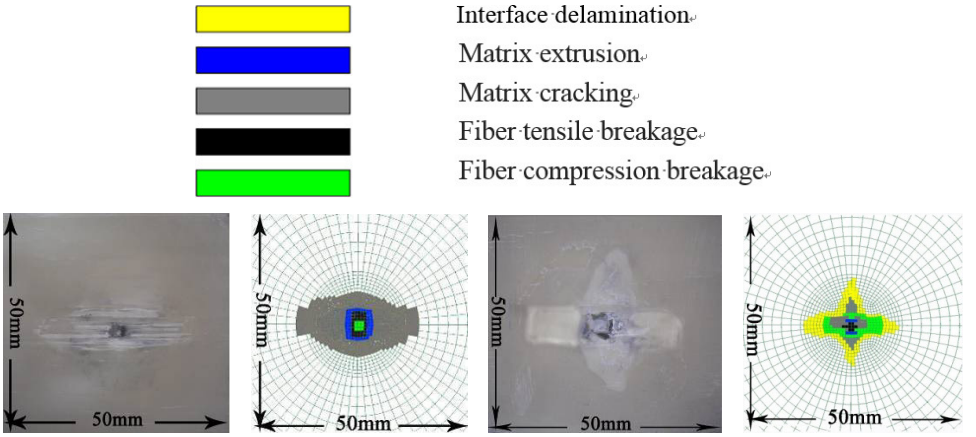

(a) (b) (c) (d)

Figure 5: The damage inside GLARE. The fiber direction of impact back is 0°, a) Al/0/0/0/0/AL specimen internal damage test photo, b) Al/0/0/0/0/AL specimen internal simulation results, c) Al/0/90/90/0/AL specimen internal damage test photo, b) Al/0/90/90/0/AL specimen internal simulation results

2.4 Damage evolution process of GLARE

In order to analyze the internal damage evolution process of GLARE, Al/0/90/90/0/Al under 25J impact is simulated. Because delamination is a significant symbol of impact damage, the change of delamination area simulation results are obtained as **Figure 6**. Simulation results show that delamination first occur between the impact back aluminum alloy sheet and prepreg, followed between impact surface prepreg layers, then between impact surface aluminum alloy sheet and prepreg.

In order to obtain the delamination evolution process, 4 moments during the impact are selected, and delamination simulation results are shown in **Figure 7**. In the simulation, the side of laminates that first touch the impactor is defined as the impact surface, and the other side is impact back. When $t = 0.125$ms, delamination occur around the contact zone between impact back aluminum alloy sheet and prepreg as shown in **Figure 7**(g1), but no delamination occur in other interfaces. When $t = 0.75$ms, delamination occur around the contact zone between impact surface 0° and 90° prepreg as shown in **Figure 7**(d2), and the delamination between impact back aluminum alloy sheet and prepreg extends out as shown in **Figure 7**(g2),

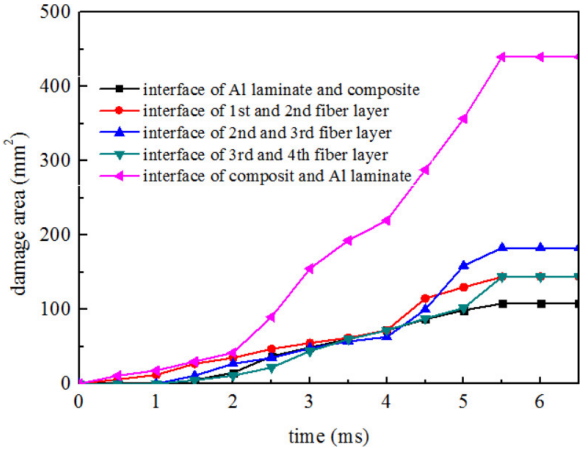

Figure 6: The interfacial delamination area with time

but no delamination occur in other interfaces. When $t = 3.75$ms, delamination occurs around the contact zone between impact surface aluminum alloy sheet and prepreg as shown in **Figure 7**(c3). Massive delamination occur between 0° and 90° prepreg as shown in **Figure 7**(d3), between 90° and 0° prepreg as shown in **Figure 7**(f3). Delamination between the impact back aluminum alloy sheet and prepreg extend in and out is shown in **Figure 7**(g3), but no delamination occur in center interface as shown in **Figure 7**(e3). When $t = 5.5$ms, delamination between the aluminum alloy sheet and prepreg extend out and in as shown in **Figure 7**(c4) and **Figure 7**(g4), and delamination between different prepreg layers are maximized as shown in **Figure 7**(d4) and **Figure 7**(f4), but no delamination in center interface as shown in **Figure 7**(e4). Simulation results show that delamination area between prepreg layers extend a lot in the bottom prepreg direction and extend a bit in upper prepreg direction, and the delamination area shape similar to an oval. This phenomenon due to the interface is be influenced by the neighbor prepregs, and the bottom pregpreg undergoes larger deformation than upper prepreg during impact, so the delamination extends a lot in the bottom prepreg laying direction, and the shape of the delamination is similar to an oval.

3 Effect of stacking sequence on impact damage of GLARE

In order to analyze the influence of stacking sequence on GLARE impact damage, the finite element model established above is adopted to simulate different GLARE under 25J impact. GLARE are Al/0/90/Al, Al/0/90/0/90/Al, Al/0/90/90/0/Al, Al/0/0/0/0/Al and Al/0/45/90/-45/Al. During the simulation, 11kg impactor with 8mm

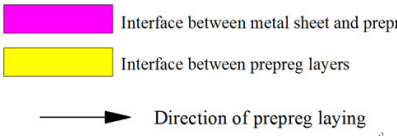

(a) Failure mode and impact back of fiber laying direction

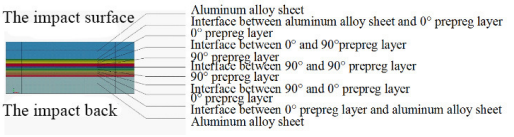

(b) Details of finite element model of GLARE

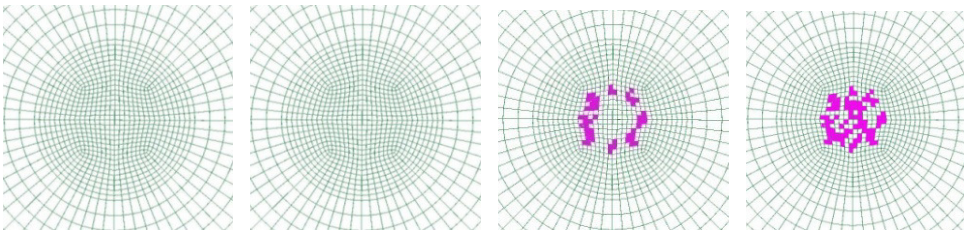

(c1) $t = 0.125$ms (c2) $t = 0.75$ms (c3) $t = 3.75$ms (c4) $t = 5.5$ms

(c) Interface between aluminum alloy sheet and 0° prepreg layer

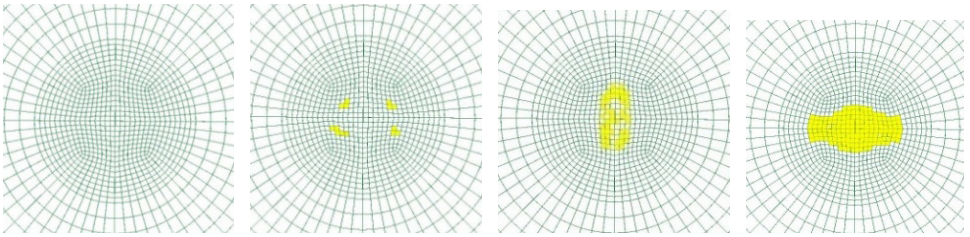

(d1) $t = 0.125$ms (d2) $t = 0.75$ms (d3) $t = 3.75$ms (d4) $t = 5.5$ms

(d) The interface between 0° and 90° prepreg layers

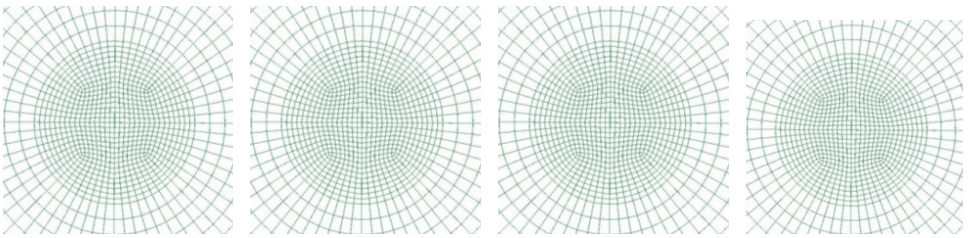

(e1) $t = 0.125$ms (e2) $t = 0.75$ms (e3) $t = 3.75$ms (e4) $t = 5.5$ms

(e) The interface between 90° and 90° prepreg layers

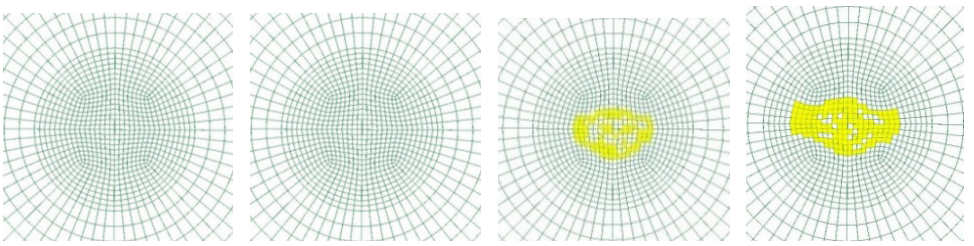

(f1) $t = 0.125$ms (f2) $t = 0.75$ms (f3) $t = 3.75$ms (f4) $t = 5.5$ms

(f) The interface between 90° and 0° prepreg layers

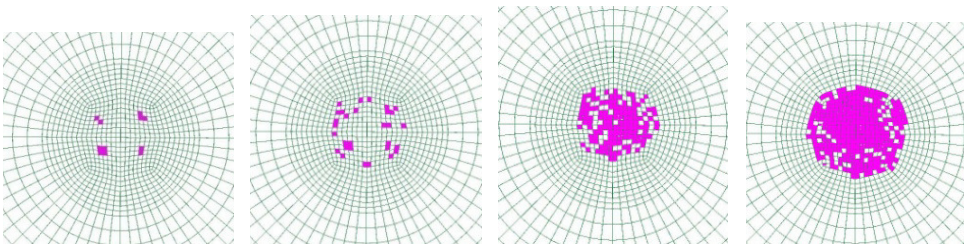

(g1) $t = 0.125$ms (g2) $t = 0.75$ms (g3) $t = 3.75$ms (g4) $t = 5.5$ms

(g) the interface between 0° prepreg layer and aluminum alloy sheet

Figure 7: Evolution of interfacial delamination inside GLARE during the impact

diameter is employed. The size of GLARE and the properties of the component materials are shown as **Table 1** to **Table 3**.

During impact, stress analytical results of each element in model is obtained, then the values are put into the equations (3)–(7) to judge the element failure mode, finally all the failure element occupy the area of the model is obtained in **Figure 8**. By comparing the simulation results of the damage area, it is found that the damage area with two-layer prepreg (Al/0/90/Al) is larger than that with four-layer prepreg, which indicates that increasing prepreg layers can increase impact damage tolerance. Comparing the damage area of GLARE with four-layer prepreg, the damage area of Al/0/0/0/0/Al is the largest, which reveals that the angle between layers can increase impact damage tolerance of GLARE. Comparing the damage area of Al/0/90/90/0/Al and Al/0/90/0/90/Al, the former induced a larger damage area, which shows that increasing the amount of angle between layers can improve impact damage tolerance of GLARE. Comparing the damage area of Al/0/90/0/90/Al and Al/0/45/90/-45/Al GLARE, the former induce a larger damage area, which

means that decreasing angles between layers can improve impact damage tolerance of GLARE.

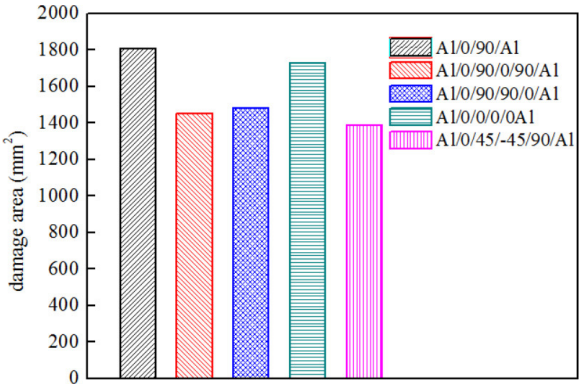

Figure 8: The change of GLARE damage area during 25J impact

4 Effect of impactor diameter on impact damage of GLARE

In order to analyze the influence of impactor diameter on GLARE impact damage, the finite element model established is adopted to simulate impacting under 25J. During simulation, the impactor is 11kg with diameters of 10mm, 12mm and 14mm respectively, and the GLARE stacking sequences are Al/0/90/Al, Al/0/90/0/90/Al, Al/0/90/90/0/Al, Al/0/0/0/0/Al and Al/0/45/90/-45/Al. Through simulating the impact process, the damage element occupy the analysis model area are obtained as **Figure 9**. The impact damage area simulation results show that damage area of GLARE reduces with the enlarging of impactor diameter. This is because the decrease of impactor diameter leads to larger local stress that GLARE is subjected to, and the damage area increases accordingly.

5 Conclusion

By combination of test and finite element simulation methods, the GLARE with orthorhombic symmetry and unidirectional stacking sequences during 25J impact are analyzed in this paper. Through modifying the composite failure criteria of Hou proposed, and combining materials performance degrade gradually method, the three-dimensional progress degradation finite element analytical model is established. The typical load-displacement curve and corrosion testing results of GLARE show that the model established is reliable.

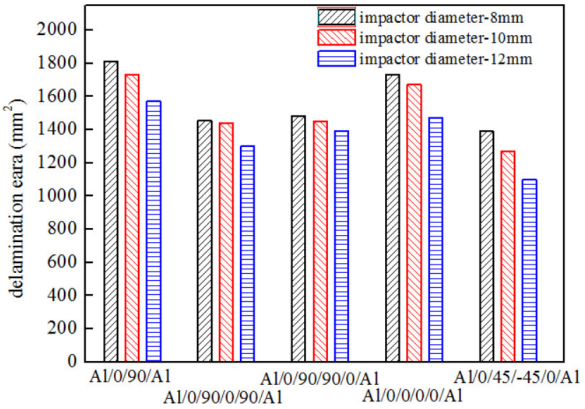

Figure 9: The change of GLARE damage area with impactor diameter

Through numerical simulation, delamination of GLARE first occur between the impact back aluminum alloy sheet and prepreg, followed between impact surface prepreg layers, then between impact surface aluminum alloy sheet and prepreg.

Through further analysis the impact damage of five GLARE by employing the finite element established, the simulation results show increasing prepreg layers can increase impact damage tolerance, and angles between layers can improve impact damage tolerance of GLARE. Damage area of GLARE reduces with the enlarging of impactor diameter.

References

Abdullah, M. R.; Cantwell, W. J. (2006): The impact resistance of polypropylene-based fibre–metal laminates. *Composites Science and Technology*, vol. 66, no. 11, pp. 1682–1693.

Chai, G. B.; Manikandan, P. (2014): Low velocity impact response of fibre-metal laminates–A review. *Composite Structures*, vol. 107, pp. 363–381.

Chai, G. B.; Zhu, S. (2011): A review of low-velocity impact on sandwich structures. *Proceedings of the Institution of Mechanical Engineers, Part L: Journal of Materials Design and Applications*, vol. 225, no. 4, pp. 207–230.

Dong, L.; El-Gizawy; A. S.; Juhany; K. A.; Atluri; S. N. (2014): A simple locking-alleviated 3D 8-node mixed-collocation c0 finite element with over-integration, for functionally-graded and laminated thick-section plates and shells, with & without z-pins. *CMC: Computers Materials and Continua*, vol. 41, no. 3, pp. 163–192.

Dong, L.; El-Gizawy, A. S.; Juhany, K. A.; Atluri, S. N. (2014): A simple locking-alleviated 4-node mixed-collocation finite element with over-integration, for homogeneous or functionally-graded or thick-section laminated composite beams. *CMC: Computers, Materials & Continua*, vol. 40, no. 1, pp. 49–77ï¿½ï¿½

Faggiani, A.; Falzon, B. G. (2010): Predicting low-velocity impact damage on a stiffened composite panel. *Composites Part A: Applied Science and Manufacturing*, vol. 41, no. 6, pp. 737–749.

Foo, C. C.; Seah, L. K.; Chai, G. B. (2011): A modified energy-balance model to predict low-velocity impact response for sandwich composites. *Composite Structures*, vol. 93, no. 5, pp. 1385–1393.

Hashin, Z. (1979): Analysis of properties of fiber composites with anisotropic constituents. *Journal of Applied Mechanics*, vol. 46, no. 3, pp. 543–550.

Hou, J. (2000): Prediction of impact damage in composite plates. *Composites Science and Technology*, vol. 60, no. 2, pp. 273–281.

Kashani, M. H.; Sadighi, M.; Lalehpour, A. (2015): The effect of impact energy division over repeated low-velocity impact on fiber metal laminates. *Journal of Composite Materials*, vol. 49, no. 6, pp. 635–646.

Kay, G. (2002): Failure Modeling of Titanium-61-4V and 2024-T3 Aluminum with the Johnson-Cook Material Model. Technical Rep. Lawrence Livermore National Laboratory, Livermore, CA.

Kermanidis, T. (2000): Finite element modeling of damage accumulation in bolted composite joints under incremental tensile loading. in *Proceedings of the Third ECCOMAS Congress*.

Lee, Y.-S.; Kang, K.-H.; Park, O. (1997): Response of hybrid laminated composite plates under low-velocity impact. *Computers & Structures*, vol. 65, no. 6, pp. 965–974.

Liu, Y.; Liaw, B. (2010): Effects of constituents and lay-up configuration on drop-weight tests of fiber-metal laminates. *Applied Composite Materials*, vol. 17, no. 1, pp. 43–62.

Pang, S. S.; Zhao, Y.; Yang, C.; Griffin, S. A. (1991): Impact response of composite laminates with a hemispherical indenter. *Polymer Engineering & Science*, vol. 31, no. 20, pp. 1461–1466.

Pierson, M. O.; Vaziri, R. (1996): Analytical solution for low-velocity impact response of composite plates. *AIAA Journal*, vol. 34, no. 8, pp. 1633–1640.

Straznicky, P. V. (2000): Applications of fiber-metal laminates. *Polymer Composites*, vol. 21, no. 4, pp. 558–567.

Sinmazçelik, T.; Avcu, E.; Bora, M.; Çoban, O. (2011): A review: fibre metal laminates, background, bonding types and applied test methods. *Materials & Design*, vol. 32, no. 7, pp. 3671–3685.

Sosa, J. L. C.; Karapurath, N. (2012): Delamination modelling of GLARE using the extended finite element method. *Composites Science and Technology*, vol. 72, no. 7, pp. 788–791.

Tita, V.; J. de Carvalho.; Vandepitte (2008): Failure analysis of low velocity impact on thin composite laminates: Experimental and numerical approaches. *Composite Structures*, vol. 83, no. 4, pp. 413–428.

Vlot, A.; Vogelesang, L.; De Vries, T. (1999): Towards application of fibre metal laminates in large aircraft. *Aircraft Engineering and Aerospace Technology*, vol. 71, no. 6, pp. 558–570.

Vlot, A. (1996): Impact loading on fibre metal laminates. *International Journal of Impact Engineering*, vol. 18, no. 3, pp. 291–307.

Vlot, A.; Gunnink, J. W. (2011): Fibre metal laminates: an introduction. *Springer Science & Business Media*.

Vogelesang; L. B.; Vlot, A. (2000): Development of fibre metal laminates for advanced aerospace structures. *Journal of Materials Processing Technology*, vol. 103, no. 1, pp. 1–5.

Wu, G.; Yang, J. M. (2005): The mechanical behavior of GLARE laminates for aircraft structures. *Jom*, vol. 57, no. 1, pp. 72–79.

Yamada, S. E.; Sun, C. T. (1978): Analysis of laminate strength and its distribution. *Journal of Composite Materials*, vol. 12, no. 3, pp. 275–284.

Zhou, J.; Hassan, M. Z.; Guan, Z. (2012): The low velocity impact response of foam-based sandwich panels. *Composites science and Technology*, vol. 72, no. 14, pp. 1781–1790.

Zhou, D. W.; Stronge, W. J. (2006): Low velocity impact denting of HSSA lightweight sandwich panel. *International Journal of Mechanical Sciences*, vol. 48, no. 10, pp. 1031–1045.